# **Journal of Rare Cardiovascular Diseases**







Non-Invasive Automatic Detection and Classification of Melanoma Skin Cancer using the Modified EfficientNetB7 Model

<sup>1</sup>Babu Kumar S, <sup>2</sup>Sowbhagya M, <sup>3</sup>Nandini G, <sup>4</sup>Pooja Nayak , <sup>5</sup>Nagarathna C R, <sup>6</sup>Anusha Preetham, <sup>7</sup>Anoop G L

Article History
Received:23.09.2025
Revised: 09.10.2025
Accepted:
21.10.2025
Published:
04.11.2025

Abstract: Skin cancer is a significant global health concern, with rising incidence rates reported in recent decades. Skin cancer falls into two basic categories: non-melanoma (benign) and melanoma (malignant). Merkel cell carcinoma and melanoma are more severe cancers, although basal cell carcinoma and squamous cell carcinoma are the most prevalent non-melanoma kinds. Advanced imaging techniques are necessary for effective therapy because early identification and categorization are critical. Enhancing algorithm accuracy in skin cancer diagnosis is mostly dependent on pre-processing procedures. Following the crucial stages of image acquisition, cleaning, enhancement, and segmentation, feature extraction is employed to extract the essential characteristics of the lesion. Data augmentation enhances the generalization of the model by including noise, rotation, scaling, and other techniques in the training dataset. The study considers skin cancer classification using the Modified EfficientNetB7 Model. EfficientNetB7 is one of the largest models in the EfficientNet series, designed for tasks that demand high accuracy and can benefit from a deeper and wider neural network. It is particularly useful for image classification tasks on large datasets [12]. While comparing the EfficientNet-B7 with other models(ARDT-DenseNet, VGG19, Stacked model, Ensembling, Inception-v3) we are getting accuracy of 96.52%, precision of 96.44%, recall value of 96.82% and F1 score of 96.3%.

Keywords: Skin Cancer, Classification, Preprocessing, Augmentation, Modified EfficientNet-B7

## **INTRODUCTION**

One of the most prevalent malignancies in the world is skin cancer. Skin cancer that does not begin as melanoma is known as non-melanoma skin tumors. The two primary types of skin cancer are melanoma (malignant) and nonmelanoma (benign). The real incidence of skin cancer is difficult to quantify because diagnostic criteria are lacking and underreporting occurs. But during the past few decades, epidemiologic investigations have revealed rising rates of both NMSC and melanoma. The head and neck are commonly the sites of skin cancer, which can cause severe morbidity during diagnosis and treatment. There are 4 main types of skin cancer:

1) Basal cell carcinoma-The rounded cells in the bottom epidermis are known as basal cells. This kind of cell is the source of around 80% of skin

- used to characterize these tumors. Rarely does this form of skin cancer migrate to other body areas and typically develops slowly.
- 2) Squamous cell carcinoma-Squamous cells, which are flat, scale-like cells, make up the majority of the epidermis. These cells give rise to squamous cell carcinomas, which make about 20% of all skin malignancies. Squamous cell carcinoma can be seen in numerous areas of the skin since it is mostly brought on by sun exposure. It can also develop on skin that has been burned, damaged by chemicals, or exposed to x-rays.
- 3) Merkel cell carcinoma-Highly aggressive or rapidly spreading, Merkel cell cancer is a rare malignancy. It originates in the hair follicles and in the hormone-producing cells under the skin. Usually, the head and neck area are affected. Another name for Merkel cell cancer is neuroendocrine carcinoma of the skin.

malignancies. Basal cell carcinomas are the term

<sup>&</sup>lt;sup>1</sup>Assistant Professor, Department of CSE, Christ University, Bangalore, India

<sup>&</sup>lt;sup>2</sup>Associate professor, Department of CSE, KSIT, Karnataka, India

<sup>&</sup>lt;sup>3</sup>Associate Professor, Department of ISE, BNMIT, Bangalore, India

<sup>&</sup>lt;sup>4</sup>Associate Professor, Department of ISE, DSATM, Bangalore, India

<sup>&</sup>lt;sup>5</sup>Associate Professor, Department of AI and ML, BNMIT, Bangalore, India

<sup>&</sup>lt;sup>6</sup>Associate Professor, Department of CSE, DSCE, Bangalore, India

<sup>&</sup>lt;sup>7</sup>Assistant Professor, School of Engineering and Technology, Christ University, Bangalore, India

Melanoma-Melanocytes, the cells that give skin its colour, give birth to melanoma, a very aggressive kind of skin cancer. If left untreated, it poses a serious threat to health because of its propensity to swiftly grow and spread to other parts of the body. Melanomas frequently appear as irregularly shaped moles of different colours and sizes, and they are associated with risk factors such prolonged sun exposure, pale skin, and a family history of the disease. Melanoma and other cancers that display invasive and possibly fatal behaviour are referred to as "malignant" more generally. Malignant tumours can spread to other organs and invade nearby tissues, posing a serious threat to one's health if they are not swiftly treated. Different skin growths, such as warts, cysts, and benign tumours like seborrheic keratosis, are included in the category of "non-melanoma benign" skin diseases. These growths are not malignant, and they usually do not spread to other tissues or infect surrounding ones. They are often not lifethreatening and may be carefully handled or removed if necessary, despite the fact that they could cause discomfort or cosmetic issues [11] [31].

The figure 1 below shows the sample Benign and Malignant Images

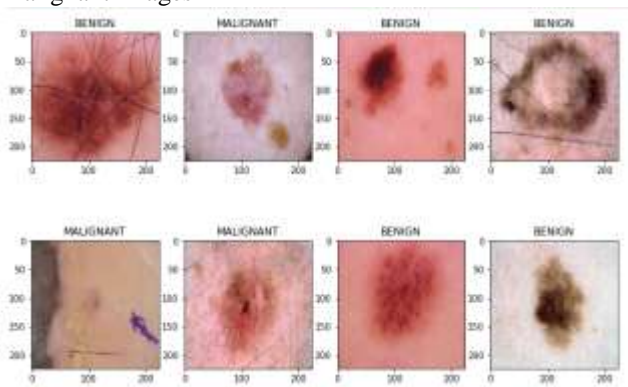


Figure 1: Sample Benign Malignant Images

Skin cancer is the type of cancer that is most common. approximated since are keratinocyte carcinoma, a kind of non-melanoma skin cancer, is so prevalent and frequently treatable. This is due to the uncommon practice of reporting individual cases to cancer registries. In the United States, 3.3 million persons have an estimated 5.4 million instances of squamous and basal cell carcinoma annually. Some patients receive more than one skin cancer diagnosis. Non-melanoma skin cancer cases have increased during the past few years. Longer life spans, more sun exposure, and faster illness identification are probably to blame for this. Squamous cell carcinoma is far less frequent than basal cell cancer. Basal cell carcinoma makes up around 80% of skin malignancies that are not melanoma. In recent years, there have been fewer fatalities from these skin malignancies. Each year, basal cell and squamous cell skin cancer claim the lives of

about 2,000 people. These skin cancers carry a greater mortality risk for older persons and those with weakened immune systems. Every year, over 7,180 people pass away from melanoma. About 4,630 individuals each year pass away from other, less frequent kinds of skin cancer. Approximately 2,000 Americans receive a Merkel cell cancer diagnosis each year in the US. The previous several decades have seen a sharp increase in this number. 90% of Merkel cell cancer diagnoses are given to white persons, and a sizable majority of patients are older than 70. The likelihood that a man will be diagnosed with the condition is double that of a woman.It is vital to keep in mind that non-melanoma skin cancer numbers are estimates. Additionally, every five years, researchers assess the survival rates for various forms of skin cancer. As a result, the estimate could not reflect the effects of earlier diagnosis or therapy that is accessible in fewer than five years [13]. Pre-processing methods improve the precision and efficiency of algorithms used in the identification and categorization of skin cancer. The process begins with Image Acquisition, where images are acquired using digital cameras or dermatoscopic devices. These images often contain imperfections like artifacts, noise, or lighting variations. Image Cleaning is used to rectify these imperfections using filters like median or Gaussian filters. Image Enhancement is then followed by Colour Normalisation, which standardises the colour representation of skin lesion images. Image Registration aligns multiple images of the same lesion, eliminating variations caused by scale, rotation, or translation differences. Image Segmentation is crucial in distinguishing lesion areas from healthy skin, using algorithms like threshold-based, region-based, or machine learning-based techniques. The Feature Extraction phase extracts relevant attributes like shape, texture, and colour from the segmented areas, encapsulating essential characteristics for skin lesion classification. These pre-processing techniques serve as a foundation for standardising, enhancing, and extracting vital information from skin lesion images, thereby enhancing the accuracy and efficacy of methods for classifying and detecting skin cancer [14].

Data augmentation is technique used for classifying and detecting skin cancer to increase the size and diversity of the training dataset, improving model generalisation and performance. Dermatology image processing employs various augmentation techniques to improve the dataset's versatility for training machine learning models. These techniques include rotation, flipping, scaling, and translation, which allow images to be adjusted to different angles and represent different skin lesions. Noise addition introduces variability in imaging conditions by incorporating random noise, contrast adjustment, elastic deformation. colour augmentation techniques. These techniques simulate noisy environments or lighting variations, and enhance the visibility of specific features. Contrast adjustment modifies image contrast, while elastic deformation introduces local deformations by displacing pixels based on random elastic distortions. Colour augmentation



techniques like hue shifting, brightness adjustment, or colour channel swapping emulate variations in skin lesion appearance and colour characteristics. A balanced approach to these augmentation techniques is crucial to prevent overfitting and ensure the dataset accurately reflects the diversity of skin lesions. It is essential to consider the dataset's specific characteristics, limitations, and domain knowledge when implementing these strategies [15].

Deep Learning has become a powerful tool for handling large data volumes, with hidden layer technology being pattern particularly popular recognition. for Convolutional Neural Networks (CNN), also known as ConvNet, are widely used for computer vision applications. CNNs consist of several layers, including the input layer, convolutional layer, pooling layer, and fully connected layers. These layers play specific roles in feature extraction and classification. The input layer receives raw image data, while convolutional layers examine the image to identify patterns, edges, and Activation layers provide non-linearity, textures. allowing the network to recognize complex correlations. Pooling layers reduce spatial dimensions while preserving essential data, improving computing efficiency. Finally, completely linked layers link neurons in different layers, making it easier to acquire high-level representations. CNNs are particularly useful in skin cancer diagnosis, providing an automated, effective, and highly accurate method for early and accurate diagnosis of malignant lesions. They can handle large datasets and support continuous learning due to their scalability and flexibility, ensuring diagnostic models keep up with changing trends in skin cancer diagnosis [16].

# 1. Related Work

Mohammad Shorfuzzaman [1], proposed an explainable CNN-based stacked ensemble architecture to identify melanoma skin cancer at an early stage. The stacking ensemble framework applies the notion of transfer learning by combining many CNN submodels that perform the same classification task. Three CNNs are used in the simulation: Xception, EffcientNetB0, and the DenseNet121 sub-models with adjusted weights. The final prediction results are generated by combining all of the sub-model predictions into a new meta-learner model. The model is evaluated using pictures of benign and malignant melanoma from an open-access dataset. An explanation that is comprehensibility-shaped adaptive has developed a method for producing a confusion matrix that displays the locations of pictures of melanoma. These are the disease's most important symptoms. This allows dermatologists to understand the model's decision in an understandable manner. Evaluation results show the suggested ensemble model's performance with accuracy (95.76%), AUC (0.957), and sensitivity (96.67%).

Jitendra V. Tembhurne et al. [2], explored a novel approach of extracting features from the images for skin

cancer detection. In order to extract the features, the method used machine learning techniques including contourlet transform and LBP histograms with a deep learning model called VGG19. The properties of these models are integrated using a voting method to get the final categorization of skin cancer. While the machine learning model processes photos using methods like Contourlet Transform and Local Binary Pattern Histogram, the deep learning model uses neural networks to extract information from images. Doctors may easily interact with the model by extending it to 2D pictures or data, 3D multimedia apps, cellphones, and online applications. The deep learning models and improved feature extraction architecture of the suggested model contribute to its high performance. On the ISIC Archive dataset, it scores better overall in test accuracy than cutting-edge methods. The suggested model achieves higher accuracy of 93% and individual recall scores of 99.7% and 86% for benign and malignant forms of cancer.

Walaa Gouda et al. [3], proposed a deep learning method convolution neural network (CNN) that was used to detect the two primary types of tumors, malignant and benign, using the ISIC2018 dataset.3533 skin lesions, including benign, malignant, nonmelanocytic, and melanocytic tumors, are included in this dataset. The images were initially enhanced and edited using ESRGAN.According to an aggregation of findings produced after several repetitions, photographs might be diagnosed using the CNN approach. Then, for fine-tuning, different transfer learning models, including Resnet50, InceptionV3, and Inception Resnet, were deployed. The Inception model's total accuracy rate in the recommended strategy was 85.7%, which is equivalent to that of competent dermatologists. The usage of ESRGAN as a preprocessing step, in addition to evaluating a range of models (designed CNN, Resnet50, InceptionV3, and Inception Resnet), is what makes this work unique and valuable.

Iftiaz A. Alfi et al. [4],introduced interpretable approach for ensemble stacking machine learning and deep learning for non-invasive melanoma skin cancer detection. Using manually constructed features, basic models (such as logistic regression, SVM, random forest, KNN, and gradient boosting machine) are trained and then utilized for level one stacking via crossvalidation. Using ImageNet data, pre-trained deep learning models (MobileNet, Xception, ResNet50, ResNet50V2, and DenseNet121) were used to perform transfer learning. Confusion matrices were produced by evaluating deep learning models after they had been assembled with different combinations and shapely adaptive explanations applied to determine which photos were more suggestive of illness.. Developing a skin lesion classifier faces challenges due to a lack of balanced public dataset and high interpretability in melanoma-related symptoms. Future research aims to improve skin lesion classification by utilising machine



learning and deep learning techniques enhancing accuracy. The ensemble model with the top rank identifies melanoma and a remarkable accuracy rate of 92.0%, and AUC score of 0.97.

Jing Wu et al. [5] proposed a densely connected convolutional network with attention and residual learning (ARDT-DenseNet) method for skin lesion classification . While using the ISIC 2016 dataset for skin lesion classification, the ARDT-DenseNet model achieves an ACC of 85.7% and an AUC of 83.7%; while using the ISIC 2017 dataset, the model achieves an average AUC of 91.8%. The method reported here considerably improves the categorization of skin lesions when compared to the state-of-the-art methodology. The model's performance is evaluated using metrics such as area under the ROC curve (AUC), sensitivity (SE), specificity (SP), accuracies in classification, average precision (AP), and specificity (ACC). The purpose of the work is to use the ARDT-DenseNet model from Pytorch to Python skin lesion classification.

Maryam Naqvi et al. [6] examined the most recent studies on deep learning techniques for classifying skin cancer. The study gives the summary of the most popular deep-learning algorithms most widely used datasets and deep neural networks for the classification of skin cancer.Deep learning algorithm-based algorithms are developed with the ultimate goal of building an AIpowered device that can identify skin cancers in actual time, assisting clinicians in the rapid and precise identification of skin malignancies. It additionally offers an overview of several deep learning architectures for the diagnosis of skin cancer, with a particular emphasis on the application of algorithmic deep learning for the classification of skin tumors. We examined the efficiency and computational expenses of the several deep learning methods covered in this review paper. The quantity of the datasets affects how good the deep learning algorithms are at identifying skin cancer. Furthermore, as images of white skin comprise the bulk of skin lesion datasets, evaluating the models based on deep learning on skin of diverse colours will cause accuracy to decrease. Future data collection efforts may collect skin tone-dissimilar data in an effort to rectify the color bias present in skin lesion databases. DenseNet201 obtained an F1-score of 0.744 and an accuracy of 82.9%, while Inthiyaz et al. used ResNet-50 to obtain an AUC of 0.87.

Aarushi Shah et al. [7] examined two automated methods: the Artificial Neural Network (ANN) and the Convolutional Neural Network (CNN). The research discovered that ANN and CNN were effective in early skin cancer diagnosis using various data sets and hybrid models, highlighting the potential for these technologies to increase skin cancer detection accuracy. The creation of more effective and precise skin cancer detecting systems, which may result in an earlier diagnosis and better treatment results, is one of the study's potential applications. Overall, this study emphasises the value of using cutting-edge technology, such ANN and CNN, to

the battle against skin cancer and demonstrates how these methods may have an influence on patient outcomes. Notably, the scientists discovered that CNN has demonstrated to ANN and other algorithms in general, since it can distinguish visual input more accurately than other neural networks. This allows it to provide better results. Accuracy obtained was 92%. Researchers and healthcare practitioners may use the thorough assessment and analysis of the most recent studies in this area to design and deploy skin cancer detection methods that are more efficient.

Shunichi Jinnai et al. [8] proposed 5846 clinical pictures of pigmented skin lesions from 3551 patients. Among the pigmented skin lesions were benign tumors (nevus, seborrheic keratosis. senile lentigo, and hematoma/hemangioma) and malignant tumors (malignant melanoma and basal cell carcinoma). Bounding-box annotations were added to the remaining pictures (4732 images, 2885 patients) to create the training dataset. Sixty-six patients were randomly selected, with one image chosen for each patient. Subsequently, they trained a faster, region-based CNN (FRCNN) with the training dataset, then assessed the model's performance with the test dataset. Additionally, after completing the same tasks, they used FRCNN to assess the diagnosis accuracy of ten dermatological trainees (TRNs) and ten board-certified dermatologists (BCDs). The accuracy of the FRCNN was 86.2% for sixclass classification, while the BCDs and TRNs had respective accuracy of 79.5% (p = 0.0081) and 75.1% (p < 0.00001). They employed twenty dermatologists to FRCNN's categorization compare the Consequently, the FRCNN's classification accuracy outperformed the dermatologists'. Using deep learning, they have created a skin cancer categorization system for lesions with brown to black pigmentation.

Atheer Bassel et al. [9] proposed a technique for classifying benign skin tumors and melanoma that relies on stacking classifiers with three folds. A total of 1000 skin pictures classified as benign and melanoma were used to train the algorithm. Thirty percent and seventy percent of the whole data set were used for testing and training, respectively. The primary feature extraction methods were Resnet50, Xception, and VGG16. The accuracy, F1 scores, AUC, and sensitivity measurements were used for the overall performance evaluation. Using deep learning, SVM, RF, NN, KNN, and logistic regression algorithms in the recommended Stacked CV approach, the system was trained in three steps. With an accuracy of 90.9%, the recommended method for Xception feature extraction outperformed the ResNet50 and VGG 16 algorithms. By refining and enhancing the suggested technique using an extensive training dataset, a dependable and sturdy skin cancer classification system may be produced. To assess performance, this study divides the dataset into three parts: 70% for training, 15% for validation, and 15% for testing. AUC score, sensitivity, F1 score, and accuracy measures are used to assess the system's performance. With 90.9% accuracy,



the suggested method of stacking CV on the Xception feature extraction mode showed dominance and promise.

Muhammad Ali Farooq et al. [10] proposed a study that focuses on skin cancer classification in preliminary stages using deep learning methodologies. There are two primary stages of the investigation. Images are preprocessed in the first stage to reduce clutter and enhance image quality. The image quality is compared before and after preprocessing procedures using different image quality measures, demonstrating that the image

quality is improved without sacrificing any quality. In the second stage, robust and accurate skin lesion classification is achieved by the application of deep learning models (Inception-v3 and MobileNet). Results from the experiment indicate a significant enhancement in both train and validation accuracy. Inception-v3 performed better in validation and was chosen to be tested on test data. 86% is stated as the final test accuracy using

Inception-v3.

Table 1: Current dataset, techniques and results for skin cancer detection

Authors	Year	Technique	Dataset	Result	
Mohammad Shorfuzzaman[1]	2021	CNN with Fusion Technique	ISIC	Accuracy (95.76%), sensitivity (96.67%), and AUC (0.957).	
JitendraV et al.[2]	2023	Contourlet Transform, Neural Networks, and logistic regression	ISIC	Accuracy 93% Recall Score of 99.7% 86%	
Walaa Gouda et al.[3]	2022	Augmentation and CNN	ISIC 2	Accuracy 83.2%	
Iftiaz A. Alfi et al.[4]	2022	Un-blinded CNN	ISIC 2018	Accuracy 92.0% AUC score 0.97	
Jing Wu et al. [5]	2020	DNN	ISIC 2016 and 2017	Accuracy of 85.7% AUC of 83.7%	
Maryam Naqvi et al.[6]	2023	DenseNet201 And ResNet- 50.	ImageNet, ISIC and HAM1000 0 dataset.	Accuracy 82.9% F1-score 0.744 AUC 0.87	
Aarushi Shah et al. [7]	2023	CNN	ISIC dataset	Accuracy 92%.	
Shunichi Jinnai et al. [8]	2020	CNN and FRCNN	Hospital 5846 clinical images of pigmented skin lesions	Accuracy 86.2%	
Atheer Bassel et al.[9]	2022	SVM, RF, NN, KNN, and Logistic regression methods	ISIC dataset	Accuracy 90.9%	



Muhammad Ali Farooq et al. [10]	2020	Deep neural Network with image preprocessing	Kaggle skin cancer dataset, ISIC dataset	Accuracy 86%
---------------------------------	------	---	--	--------------

## 2. Proposed Model



Figure 2: Proposed model

The above Figure 2 shows the flow diagram of the proposed model

- Data Acquisition: To create machine learning models that are accurate and dependable, collecting data on skin cancer and classifying it into benign and malignant categories is essential. The procedure involves gathering a variety of sample datasets covering a range of skin lesion kinds, guaranteeing that the model will perform effectively in real-world situations.
- Data preprocessing is essential for training machine learning models and ensuring accurate data analysis. It involves addressing issues and formatting data appropriately for the specific task. Techniques used in data preprocessing include rescaling, shuffling, and normalization to enhance, purify, and adjust the quality of the dataset.
- Image augmentation is particularly valuable because of the variety in lesion appearance and the settings in which photos are taken. It's primary goal is to modify the original photos in several approaches to synthetically broaden the training dataset's variety, which will strengthen the generalisation and durability of the machine learning models. Rotation, shrinking and cropping are the different image augmentation techniques used in skin cancer classification [17].
- Sampling depicts the dataset containing melanoma images of malignant and benign skin cancer split into training and testing (80% training data and 20% testing data) dataset [30].
- Automated feature extraction is a essential stage in skin cancer classification, converting medical images into a more understandable representation. It uses algorithms to identify and record unique patterns, traits, or representations in the data. Deep learning

- architectures can extract hierarchical and abstract characteristics directly from the input data, eliminating the need for predetermined features. Automated feature extraction improves machine learning models' efficiency, leading to better generalization and prediction performance across various datasets [18].
- This study used a modified EfficientNet-B7 model for skin cancer detection, known for its superior image classification performance. The network's upper layers were specifically designed to meet the needs of classifying skin cancer into benign and malignant groups. We sought to improve the model's capacity to identify complex patterns and traits of different skin lesions by optimizing it and adding more layers.
- Classification involves the process in which the modified EfficientNet-B7 model divides the image dataset into two categories of benign and malignant.
- The skin cancer classification model was accessed utilizing an extensive collection of metrics, including accuracy, precision, recall value, and F1 score. Accuracy measures the model's overall performance, determined by calculating its ratio of real positive predictions to all predicted positives. indicating its ability to minimize false positives and identify accurate malignant or benign cases. Precision measures the model's sensitivity to detecting genuine positives, indicating its capacity to catch all real positive cases. The F1 score provides an accurate assessment by considering a harmonic mean of recall and accuracy, and both false positives and false negatives. The model's capacity to discriminate between benign and malignant lesions was thoroughly assessed thanks to this multidimensional assessment approach, which produced well-informed conclusions [19].



# **MATERIAL AND METHODS**

The section on Materials and Methodology provides a comprehensive outline that includes the study methodology, dataset selection, algorithm selection, and preprocessing methods. Research on skin cancer detection is advanced by the use of picture augmentation and the implementation of deep neural network models, particularly a modified EfficientNet-B7. This section summarises the essential components for a thorough comprehension of the study and acts as a fundamental guide for the experimental framework.

# Algorithm

# Algorithm 1: Proposed model's (Skin Cancer classification) algorithm

//Define label for testing  $x_test,y_test=test_data.classes$  //Define classification data  $C_L \leftarrow Diff(predicted label,true label)$  Make prediction of classes Return  $C_L$  value $(P_t, G_t, N_t, M_t)$   $C_m = confusion_matrix(x_test,y_test)$  return  $(C_m)$  return  $(V_{acc})$ 

# 4.1 Dataset

As the primary input for these sophisticated learning methods, data is the cornerstone of deep learning. Since cancer is a unique disease, several datasets have been created on it. Lesion photos from publicly available image databases of known afflicted patients were used in this investigation. More specifically,the Skin Cancer Detection 2018 dataset from the International Skin Imaging Collaboration (ISIC) was utilized in the technique. The ISIC International Skin Imaging Collaboration is a collaboration between academics and business that aims to make it easier to apply digital skin imaging to help reduce melanoma mortality 10,015 photos were used for training and 1,512 images were used for testing, making a total of 11,527 images in this dataset. The training set received ground-truth data entirely from the ISIC 2018 dataset, which classified pictures into seven classes: benign keratosis, dermatofibroma, vascular lesions, basal cell carcinoma, squamous cell carcinoma, melanoma, and melanocytic nevus [20].

Another crucial step in the research cycle was separating

the dataset into sets for training, testing, and validation.. Training a Convolutional Neural Network (CNN) model, pre-trained models (ResNet, Inception, and Inception ResNet) fine-tuning, model parameter adjustments (freezing layers, learning rate, epochs, batch size), computation of multiple performance metrics (ROC, F1, AUC, recall, and confusion matrix) within the framework of the Visual Performance Metrics (VPM), and comparison of the outcomes with previous research were the next steps. The ISIC 2018 Image Dataset's importance as a strong and complete resource for improving state-of-the-art in the detection of skin cancer is highlighted by its dependence on it. The ISIC Skin Cancer Detection Dataset's Kaggle version was used for this investigation [21].

# 2.2 Preprocessing

Techniques used in data preprocessing include rescaling, shuffling, and normalization to enhance, purify, and adjust the quality of the dataset.

• Rescaling refers to bringing all the image pixel intensities to a common scale. This is crucial because different lighting conditions and camera setups might induce biases and make it more difficult for the model to identify generalizable features. Common rescaling techniques are z-score scaling, which centres data around the mean with a standard deviation of 1, and min-max scaling, which scales values to a range between 0 and 1. Instead of being impacted by fluctuations in pixel intensity brought on by outside influences, the model may concentrate on the significant variables in the photos, such as the texture and colour of the lesions, by rescaling the pic.

$$X_{rescaled} = \frac{(v - v_{min})}{(v_{max} - v_{min})} \times max_{new} - min_{new} + min_{new}$$
(1)

The equation 1 shows the mathematical equation of rescaling.

Shuffling involves Randomizing the sequence of data points in the training set. This is important as the model must not acquire any patterns or correlations based on the order in which the data is presented. To illustrate, if all the benign lesions are shown first, followed by all the malignant lesions, the model may solely associate the order with the class, rather than comprehending the distinct features that differentiate benign from malignant lesions. Shuffling guarantees that the model learns from the complete dataset in an impartial manner and can apply its knowledge to novel, unseen data.

 $shuffled_{image(i,:)} =$   $original\_image(permutation(1: M))$ 

rstematic of laster

(2)

 $shuffled_{image(:,J)} =$   $original\_image(permutation(1:M),J)$  (3)

The equation (2) and (3) shows the mathematical equations of shuffling the rows and columns of image.

• Normalisation addresses the problem of varying scales and distributions among different features. This can pose challenges during the training phase, as features with larger scales or wider distributions may have a greater influence on the learning process. By utilizing normalization techniques such as L1 norm and L2 norm, all features are brought to a standardized scale, guaranteeing equal contribution from each feature in the learning process. This enhancement leads to improved accuracy of the model and eliminates any bias towards features with larger scales.

$$v' = \frac{(v - v_{min})}{(v_{max} - v_{min})}$$

(4)

The equation (4) shows the mathematical equation of normalisation [22]

# 2.3 Image Augmentation

In computer vision and machine learning, image augmentation is a widely used approach to artificially increase the variety of a training dataset. The robustness and generalization of a machine learning model may be enhanced by creating fresh training examples by transforming the original pictures in different ways. Several popular methods for enhancing images are as follows:

 Image rotation is a frequently employed operation. It involves rotating a picture to change its orientation. The image can be rotated clockwise or counterclockwise, causing it to appear to turn to the right or left. Here we have rotated the image at 80,30 and 180-degree angles.

$$x' = x\cos\theta - y\sin\theta$$
(5)

 $y' = x sin\theta + y cos\theta$ 

The equations (5) and (4) shows the

mathematical equations of image rotation along the coordinates (x, y)

• Flipping describes the process of flipping an image's pixel spatial arrangement. There are two primary kinds of flips that arise from applying this technique along a certain axis: Horizontal Flip and Vertical Flip. An image is flipped along a vertical axis in a horizontal flip, which is also referred to as a left-right or horizontal mirror. As a result, the image's left side becomes its right side and vice versa. It is represented by a y-axis flip. An image is flipped along a horizontal axis in a vertical flip, also referred to as an up-down or vertical mirror. As a result, the image's top becomes its bottom and vice versa. It is represented as an x-axis flip.

$$x' = width - x - 1$$

(7)

$$y' = height - y - 1$$

(8)

The equations (7) and (8) shows the mathematical equations of flipping the image along the coordinates(x, y)

• Gaussian Blur is a widely used image filtering method in computer vision and image processing is called Gaussian blur. It is called after the Gaussian function, a mathematical formula that determines its shape. A kind of low-pass filter called a Gaussian blur smoothens a picture by lowering high-frequency noise and features. Convolution of the image with a Gaussian kernel, a two-dimensional bell

$$G(x) = \frac{1}{\sqrt{2\pi\sigma^2}}e^{-\frac{x^2}{2\sigma^2}}$$

(9)

(x,y) are the coordinates of a pixel in the kernel.  $\sigma$  is the standard deviation of the Gaussian distribution, controlling the width of the bell curve

The equation (9) shows the mathematical equation for Gaussian blur

• Cropping is a typical image processing technique is called cropping, which includes removing the remaining portion of a picture and keeping only a rectangular region of interest (ROI). This technique is similar to framing a picture, when concentrating on a certain region or subject. Cropping may be used to extract certain characteristics, resize a picture, and remove undesirable backgrounds, among other things. The center crop technique is a popular cropping technique that involves selecting the

(6)

image's core area. This is frequently utilized to provide a balanced viewpoint by concentrating on the primary topic or point of interest. Random Crop is a technique in which a random rectangular area from the image is chosen. This is especially helpful for adding variety and avoiding overfitting in data augmentation used in machine learning training. In fixed cropping, a certain area of the image is chosen using predetermined dimensions or coordinates. When cropping several photos consistently is necessary, this approach is used.

(10) 
$$x' = \max(\min(x, x_{end}), x_{start})$$
$$y' = \max(\min(y, y), y_{start})$$

(11)

The equation (10) shows mathematical equation of cropping of image along (x,y) coordinates

In the above equations (x', y') are the coordinates after cropping and (x,y) are the original coordinates. The coordinates  $(x_{start}, y_{start})$  and  $(x_{end}, y_{end})$  respectively represent the top-left and bottom-right corners of the rectangular region you want to retain, defining the boundaries for image cropping.

Shrinking is the process of reducing the size of an image while maintaining its aspect ratio. This is achieved through techniques such as bilinear interpolation or nearest neighbour interpolation. By shrinking the image, new variations of the original image are created, which can be used to train machine learning models. The model is exposed to a greater variety of potential skin lesion appearances during this phase, which strengthens it and increases its capacity for generalisation. Shrinking the images generates additional training data points from the existing ones which inturn effectively expands the dataset and enhances the model's ability to learn features that can be applied to a broader range of cases. Training the model on shrunken images reduces its sensitivity to variations in image size. Consequently, the model improves its ability to identify skin lesions in the original picture, regardless of their size.

$$x' = s. x \tag{12}$$

$$y' = s. y \tag{13}$$

The equations (12) and (13) represents the mathematical equations of image shrinking In the above equation (x', y') are the new coordinates after shrinking. (x, y) are the original coordinates and s is the scaling factor [23]. The Figure 3 below shows the sample

Augmented Images.

Reduced 100.00.21 Value of 00.11 Support 100.40.2 Support

Figure 3: Augmentation layer output

## 4.4 Deep Neural Network

A type of artificial neural network with numerous layers (deep architecture) between the input and output layers is called a deep neural network (DNN). Interconnected nodes, or neurons, make up each layer, and via training, the network discovers hierarchical representations of the data. DNNs are effective at recognizing intricate patterns and features in huge datasets, which makes them useful for tasks like speech recognition, image recognition, and natural language processing. Benefits include greater performance in managing complex relationships within the data, automatic feature extraction, and flexibility to various data [24].

#### 4.4.1 Convolution Neural Network

Convolutional Neural Networks (CNNs) are a specialized type of deep neural network used to handle structured grid data, such photographs. Convolutional layers are a tool used by CNNs to automatically and effectively extract hierarchical features from input data, allowing them to capture spatial patterns and hierarchies. They are particularly good at picture-related activities like object recognition and image categorization because they can see local patterns and spatial correlations. CNNs use pooling layers and shared weights to improve translation invariance and lower computing complexity. Because this design works so well with grid-like data structures, it is frequently used in computer vision [25-27].

## 4.4.2 EfficientNet:

EfficientNet is a class of convolutional neural network created to achieve the best possible balance between computational efficiency and accuracy. EfficientNet is a model size and performance balancer that produces state-of-the-art performance by consistently scaling network dimensions. It presents a compound scaling technique that effectively strikes a balance between depth, width, and resolution to deliver strong performance on a variety of tasks, making it a well-liked option in settings with limited resources.

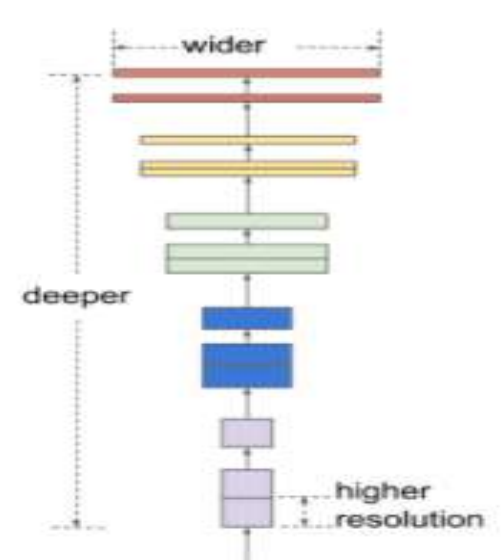


Figure 4: EfficientNet-B7

The figure 4 illustrates the compound scaling method in EfficientNet is a convolutional neural network architecture designed for image classification tasks. It aims to maintain computational efficiency while achieving high accuracy. The model has three axes: wider, deeper, and higher resolution. Previously, scaling these dimensions separately may lead to decreased benefits. However, the compound scaling approach uses predefined coefficients to scale all three dimensions proportionately. A grid search is used to identify ideal coefficient combinations, balancing efficiency and accuracy. This method allows EfficientNet models to outperform earlier models and achieve state-of-the-art performance while being smaller and quicker [32-35].

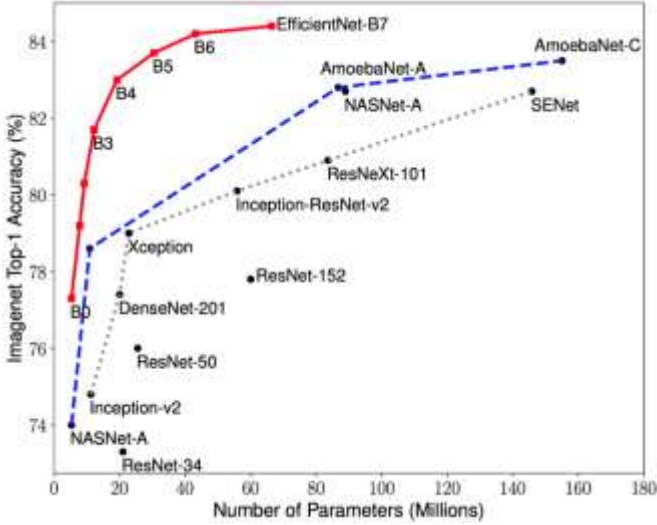


Figure 5: Model Size vs. ImageNet Accuracy.
Source: EfficientNet: Rethinking Model Scaling for
Convolutional Neural Networks

The graph in figure 5 depicts the accuracy of different versions of modified EfficientNet-B7 for image classification on the ImageNet dataset. The red line represents different versions of modified EfficientNet-B7 model, the blue line represents different versions of AmoebaNet-C, and the white dotted line represents

different versions of SENet. It reveals a relation between accuracy and model size. The smaller models with fewer parameters are less accurate and larger models with more parameters are more accurate. However, larger models are more likely to be overfitting, because they retain too much training data and struggle to generalize to new data.

The graph shows several models, including EfficientNet-B0, EfficientNet-B1, EfficientNet-B2, EfficientNet-B3, EfficientNet-B6. EfficientNet-B4. EfficientNet-B5. EfficientNet-B7. AmoebaNet-A. AmoebaNet-C. NASNet-A, SENet, Inception-ResNet-v2, Xception, ResNet-152. DenseNet-201. ResNet-50. Inception-v2. NASNet-A, and ResNet-34. EfficientNet-B7 is the most accurate model, with an accuracy of 84.4% and 87.5 million parameters.It is not as accurate as EfficientNet-B7, but it is much smaller and faster to run. This graph demonstrates that high accuracy can be achieved with the Modified EfficientNet-B7 model and is suitable for our research [36-38].

# Layers to EfficientNetB7

• Convolutional Layer- This layer works best for tasks like picture recognition since it is built to identify local patterns and characteristics in the incoming data. The layer is made up of a collection of learnable filters, also referred to as convolutional or kernel filters. These filters are tiny, spatially confined matrices that usually operate like sliding windows to scan the incoming data. Every filter is applied to the input data during the convolution procedure, and a dot product between the filter and the local area of the input it is now covering is calculated at each step. This process is used consistently across the input to produce a feature map that emphasises the existence of particular features or patterns.

$$O = \frac{W - K + 2P}{S} + 1$$
(14)

The equation (14) shows the mathematical representation of convolutional layer, where O is the output size, W is the input size, K is the filter size, P is the padding and S is the stride.

Pooling Layer - Max pooling is a down sampling technique that determines the largest value from a set of nearby pixels inside a designated area (kernel). In order to provide translation invariance and lower computational cost, it is frequently employed in CNNs to extract the most crucial information from the input. By keeping the salient characteristics in each zone, it contributes to the achievement of spatial invariance. As a result, the input's spatial dimensions are reduced, freeing up later layers to concentrate on higher-level information



$$O = \frac{W - F}{S} + 1 \tag{15}$$

The equation (15) shows the mathematical representation of pooling layer, where O is the output size, W is the input size, F is the pool size, and S is the stride [39-40].

#### 4.4.2 Modified EfficientNetB7

The modified EfficientNet-B7 architecture in the image adds convolutional layers, average pooling layers, and fully-connected (FC) layers to the original design in an effort to improve the model's accuracy for particular tasks.

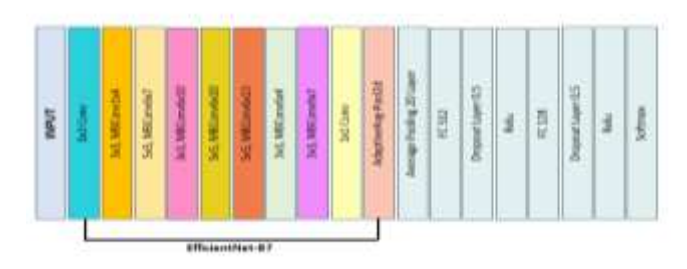


Figure 6: EfficientNet-B7 with added layers(Modified EfficientNet)

The figure 6 illustrates EfficientNet-B7 with added layers in which the input layer is on the left of the figure, while the output layer is on the right, illustrating the many network layers. Input layer takes an image as input.3x3 convolutionl layer gives the input image a 3x3 convolution filter. This aids in identifying features inside the image. The EfficientNet-B7 model has many MBConv layers, each with a unique kernel size, expansion ratio, and number of output channels. To attain great accuracy at minimal computational cost, the MBConv layers combine pointwise and depthwise separable convolutions. AdaptiveAvgPool2d layer minimises the feature maps' spatial dimensions derived from the MBConv layers. Fully-connected layers called FC layers are used to categorise images into one of a thousand groups. To avoid overfitting, dropout layers arbitrarily remove a portion of the network's neurons. Relu layers add non-linearity to the network by using the rectified linear unit (ReLU) activation function. Softmax layer outputs the probability distribution of the image belonging to each of the 1000 categories.

# Layers of the Modified EfficientNetB7

#### Dropout

In neural networks, the dropout operation is a straightforward efficient regularisation and technique. Dropout provides a degree of randomness to the training process by "dropping out" (or arbitrarily setting a portion of the input units, or at each update. This enhances neurons). generalisation and prevents any one neuron from becoming heavily dependent on the availability of certain input neurons during training. Dropout can't rely too much on any one pathway across the network, which forces it to learn more resilient and generalizable traits[41-43].

The dropout rate, often represented by p, is the proportion of units that drop out. The following equations (16) and (17) is a mathematical expression for the dropout:

During training:  $output = input \times mask$  (16)

During testing:  $output = (1 - p) \times input$  (17)

The mask is a binary vector that has the same form as the input during training, with elements assigned to 0 with probability p and 1 with probability 1-p. In testing, the input is scaled by 1-p in order to maintain the predicted output. The dropout is disabled.

#### • Activation Function-Relux

The rectified linear unit (ReLU) is an activation function that addresses the vanishing gradients problem and adds the non-linearity attribute to a deep learning model. It understands the portion of its argument that is positive. As an activation function for deep learning, it is among the most often used ones. ReLU was not differentiable at the point zero, which is the major reason it wasn't employed until lately. Differentiable functions like sigmoid and tanh were often used ReLU, on the other hand, is presently thought to be the ideal activation function for deep learning.

$$f(x) = \begin{cases} 0, for x \le 0 \\ x, for x > 0 \end{cases} = \max\{0, z\} = x1_{x>0}$$
(18)

$$f'(x) = \begin{cases} 0, for x \le 0 \\ 1, for x > 0 \end{cases} \quad (0, \propto)$$
(19)

The equations (18) and (19) shows the mathematical equations for ReLU activation function.

#### Softmax

Neural network topologies include the softmax layer, particularly when handling multi-class classification issues. The softmax function, which is positioned at the output layer, converts the raw scores or logits that the previous layers produced into a probability distribution over many classes. The model is able to assign likelihoods to each class and create a probabilistic forecast thanks to this distribution.

Given a vector of raw scores or logits z = [z1, z2, ..., zn], the softmax function calculates the probability softmax  $(z)_i$  for each class i using equation (20):

Softmax 
$$(z)_i = \frac{e^{zj}}{\sum_{j=1}^n e^{zj}}$$
 (20)

# 3. Experiment Results

This section describes the experimental set up and explores the Modified EfficientNet-B7 model in skin cancer detection through experiments conducted on the ISIC dataset. The dataset, containing pictures of both benign and malignant skin lesions. A confusion matrix is used in performance evaluation, and important measures including accuracy, precision, recall, and F-score are used to evaluate how well the model classifies data. The findings, which are depicted in Figure 7, offer information on the outcomes of detection and classification, which is essential for improving the ability to diagnose skin cancer.

# 5.1 Experimental Setup

Experiments were conducted on the ISIC dataset to illustrate the effectiveness of the Modified EfficientNet-B7 model in detecting skin cancer. Variable Setting and Experimental Assessment Index: Simulations using the ISIC dataset were run in order to compare the findings to the state of the art at the time and show how well the performed. The tensorflow Keras software for the current scheme was tested on a Windows PC equipped with Intel(R) Iris(R) Xe Graphics and 8GB of RAM. As seen in Figure 7, training and testing sets were divided in an 70% to 30% ratio. There were 1750 benign and 1751 malignant photos in the training set, and 758 benign and 708 malignant images in the testing set. Eighty percent of the lesion photos in the recommended training set were randomized. This set was used for all testing. During the learning phase, 10% of the data were then utilized for verification. Retained were the weight combinations that yielded the highest accuracy ratings.

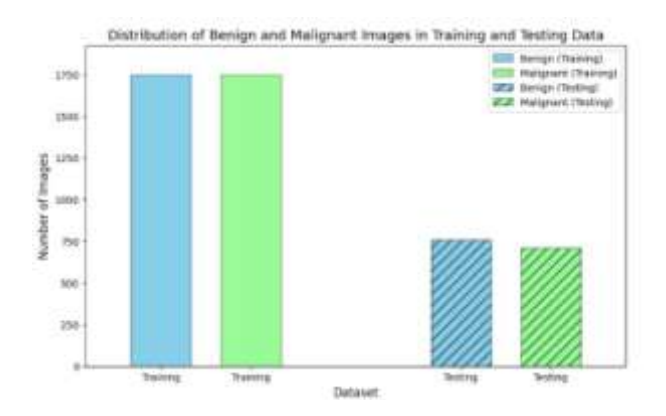


Figure 7: Distribution of dataset

#### 5.2 Performance Metrices

A numerical matrix that shows a model's confusion spots is called a confusion matrix. An organized way to relate the predictions to the original classes that the data belongs to is to use a confusion matrix. Stated differently, it represents the predicted accuracy of a classification model distributed across classes. In addition to making it possible to compute the accuracy of a classifier, either globally or class-wise, the confusion matrix also assists in the computation of other important metrics that developers often use to evaluate their models. A confusion matrix created for the same test set of a dataset but with different parameters is used to evaluate the relative advantages and disadvantages of several classifiers and make assumptions about how to combine them (ensemble learning) to attain the best performance. A dataset with just two unique categories of data is called a binary class dataset. To keep things simple, we might refer to these two groups as the "positive" and the "negative."

- True Positive (TP): The number of cases that were accurately forecasted as positive. Stated otherwise, these are the situations where both the actual class and the model's prediction are positive.
- True Negative (TN): The quantity of cases that were accurately anticipated to be negative. That is, these are the situations where the actual class is likewise negative, notwithstanding the model's negative prediction.
- False Positive (FP): The number of cases that were erroneously counted as positive. Stated otherwise, these are the situations in which the model yielded a positive prediction, but the actual class is negative.
- False Negative (FN): The number of cases that were erroneously counted as negative. Stated otherwise, these are the situations in which the model yielded a negative prediction, while the actual class is positive. Figure 8 shows the sample confusion matrix format. Figure 8 shows the sample confusion matrix format.



# **Actual Values**

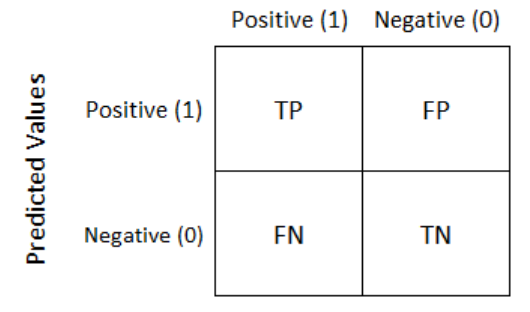


Figure 8: Confusion Matrix

Using confusion matrix, the various performance assessment metrics is calculated to verify the performance of the proposed model. An extensive discussion of the evaluation metrics used and their results is provided in this section of the study. The main metric for assessing classification efficiency is classifier accuracy (Acc). It is defined as the number of examples (images) in the dataset under investigation divided by the number of instances (images) that were correctly classified in Equation (21). Precision (Pr) and recall (Rc) are the two measures that are typically used to assess how well image classification algorithms work. Equation (22) expresses precision as the ratio of accurately identified classed shots to the total number of images. Equation (23) states that recall is the proportion of successfully classified photos in the database to the total number of linked images. The harmonic mean of accuracy and recall is the F-score; a higher number indicates the system's predictive capacity. Systems' efficacy cannot be determined just by their recall or The F-score (Fs) is represented accuracy. mathematically by equation (24) where  $T^{p}$  indicates a true positive,  $T^n$  indicates a true negative,  $F^p$  indicates a false positive, and  $F^n$  indicates a false negative [28].

$$Acc = \frac{T^p + T^n}{T^p + T^n + F^p + F^n}$$
 (21)

$$Pr = \frac{T^p}{T^p + F^p} \tag{22}$$

$$Rc = \frac{T^p}{T^p + F^n} \tag{23}$$

$$Acc = \frac{T^{p} + T^{n}}{T^{p} + T^{n} + F^{p} + F^{n}}$$

$$Pr = \frac{T^{p}}{T^{p} + F^{p}}$$

$$Rc = \frac{T^{p}}{T^{p} + F^{n}}$$

$$Fs = 2 \times \left(\frac{Pr \times Rc}{Pr + Rc}\right),$$
(21)
(22)

# **5.3 Sample Results**

In the context of skin cancer detection, a false positive happens when a benign case is predicted to be malignant by the model. While it is allowed, medical professionals should examine it carefully. Accurate forecasts of benign instances are represented by true negatives. True positives demonstrate the validity of the model by accurately identifying situations that are malignant.

However, false negatives, where the model predicts benign for a malignant case, are especially important since they run the danger of malignant cancers, which call for more care and attention.

- False positive: Actual benign, predicted malignant (but it is still acceptable since doctors would pay careful attention on it)
- True negative: Actual benign, predicted benign (means correct prediction)
- True positive: Actual malignant, predicted malignant (means correct prediction)
- False negative: Actual malignant, predicted benign (This is the most dangerous case since we would not want a Malignant Cancer to get unnoticed or given less attention)

The Figure 8 shows the skin cancer detection results.

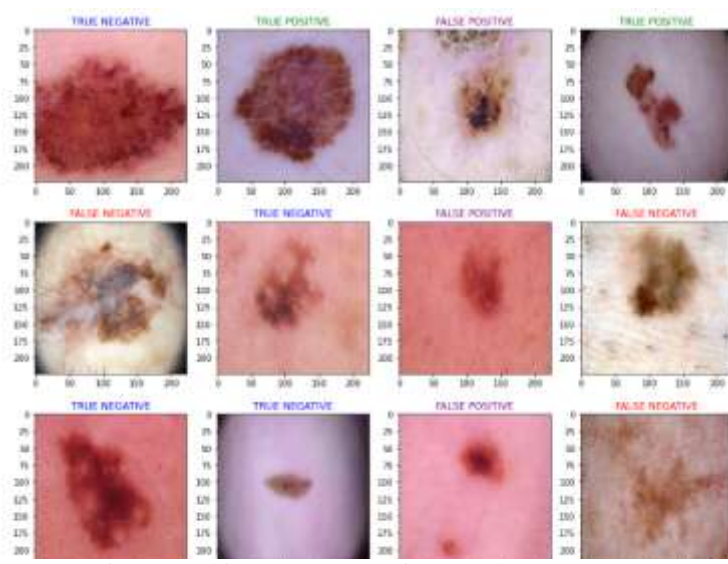


Figure 9: Skin Cancer Detection Results

# **Statistical Analysis**

This section explores the efficiency of a Modified EfficientNet-B7 model for skin cancer detection by contrasting its performance with cutting-edge methods. Table 1 presents the improved accuracy, precision, recall, and F1-Score of the suggested model in comparison to current methodologies. Figures 8, 10, and 11 also show the model's accuracy, training and validation progress, and loss dynamics. Figures 12 and 13 show confusion matrices, which provide an additional perspective of the model's performance in differentiating between benign and malignant lesions. Ultimately, this comprehensive evaluation highlights the promising potential of the proposed model in improving skin cancer diagnostic capabilities.

# 6.1 Training Accuracy and Loss

The graph in figure 14 compares the accuracy, recall, F1 score and precision of five different neural network models with proposed model for skin cancer detection. It

reveals that the Modified EfficientNet-B7 routinely outperforms other models but when compared to the stacked model, there isn't much of a difference in accuracy and precision because it makes use of redundant or overly complex CNN layers. However, the proposed model with less complex layers and better architectural decisions performs better than the Stacked model while consuming less energy. Faster processing is possible without compromising feature capture due to its streamlined architecture and thinner layering. For a lower computational cost while retaining acceptable feature extraction, it could make use of smaller kernels or effective activations. With fewer parameters and a smaller size, it requires less energy to maintain precision. Furthermore, Modified EfficientNet-B7 could important characteristics via attention prioritize processes.

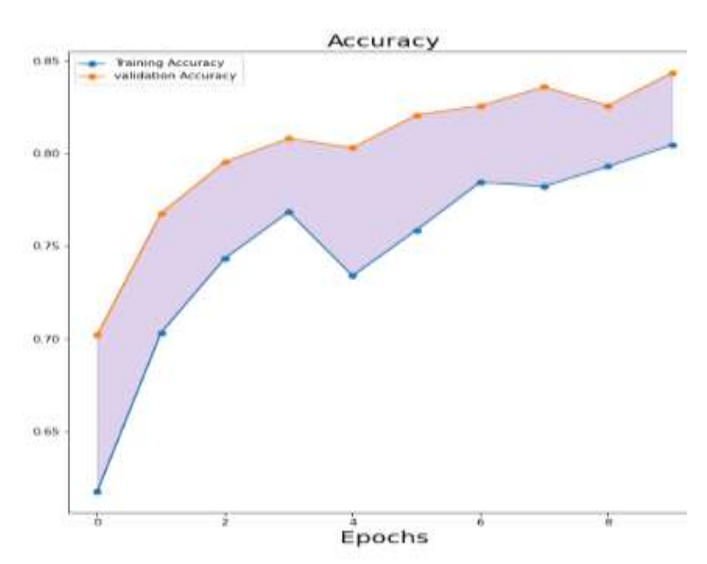


Figure 10: Accuracy graph of training and validation

The line graph in figure 10 shows the training and validation accuracy of a skin cancer detection model as the number of training epochs increases. The model gains knowledge gradually from the training data, while the validation accuracy also rises, although at a slower pace than the training accuracy. This shows that the model is adequate given the data for two reasons: it can learn generalizable features related to skin cancer detection and there is no significant difference between the training and validation curves, indicating it is learning transferable patterns. This figure provides evidence for the model's data adequacy and potential in skin cancer detection tasks, although further research and performance testing on bigger datasets are required.

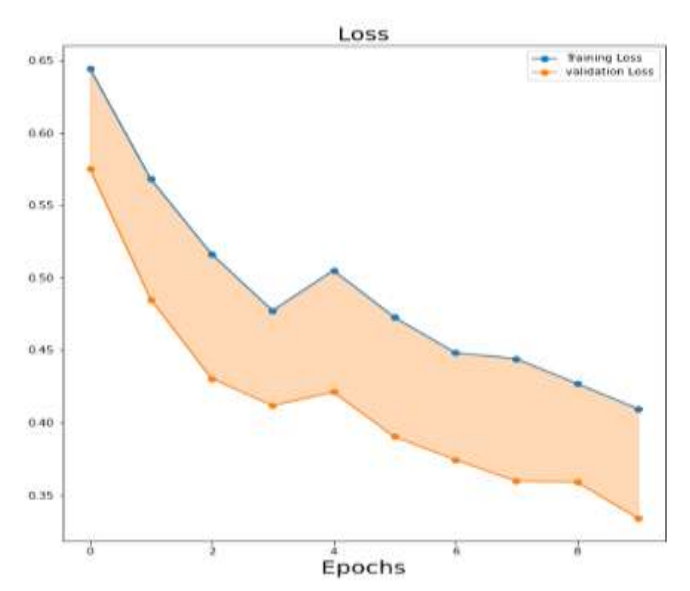


Figure 11: Graph showing training and validation loss

The graph in figure 11 illustrates the training loss and validation loss of Modified EfficientNet-B7 for skin cancer detection as the number of training epochs increases. The blue line represents the training loss and the orange line represents the validation loss. The objective is to train a model with low training and validation loss, ensuring precise prediction of both training and unseen data labels. The training loss decreases gradually with increasing training epochs, indicating the model's learning from the training data and improving its ability to predict correct labels. However, there is a minor drop in the validation loss, indicating that the model overfits the training set and has difficulty generalizing to new data. In spite of this, the model's training and validation losses both decline, suggesting that it has received sufficient data to train and is capable to learn important features for skin cancer detection. The model's strong capacity to generalize to new data is suggested by its low validation loss. The model's performance on unseen data is promising, but further refinement is needed to enhance its effectiveness [41-45].

# 4.2 Detection and Classification Results:

Using Modified EfficientNet-B7, the confusion matrices of the benign and malignant cancer results are displayed in Figures 9 and 10. While 24 malignant images were incorrectly labelled as benign and 27 benignly infected images were misconstrued as malignant, 731 benign images were correctly diagnosed as benign, and 684 malignant images were correctly diagnosed as malignant.

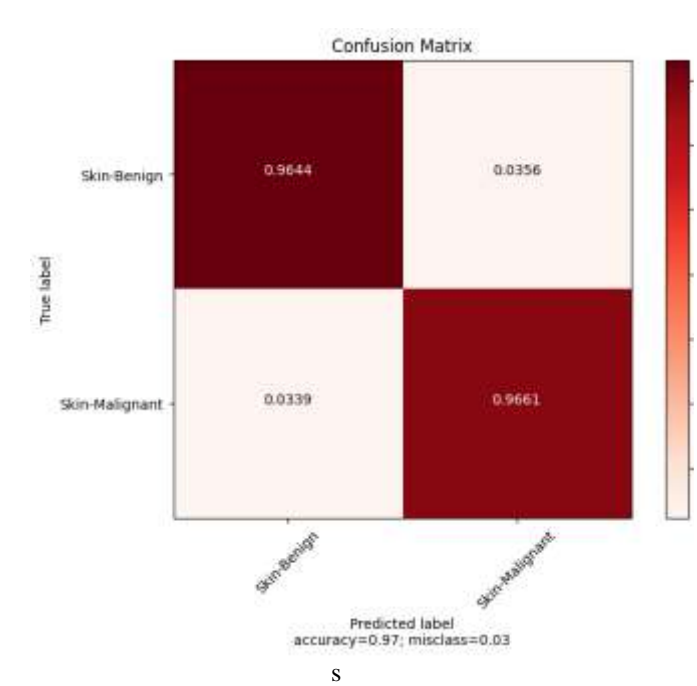


Figure 12: Normalized confusion matrix representation of benign and malignant classification

The confusion matrix in figure 12 shows the performance of the model which is classifying skin lesions as either benign or malignant. Since the matrix has been normalized, the values no longer reflect raw numbers but rather percentages. The accuracy of the model for each class is displayed in the diagonal cells of matrix: Malignant lesions were accurately categorized as 96.61% of the time, whereas benign lesions were correctly diagnosed as 96.44% of the time. The model's error rates are displayed in the off-diagonal cells: 3.39% of malignant lesions were incorrectly categorized as benign, while 3.56% of benign lesions were incorrectly labeled as malignant. Over all the model is performing well, with a high accuracy rate and low error rates for both benign and malignant lesions.

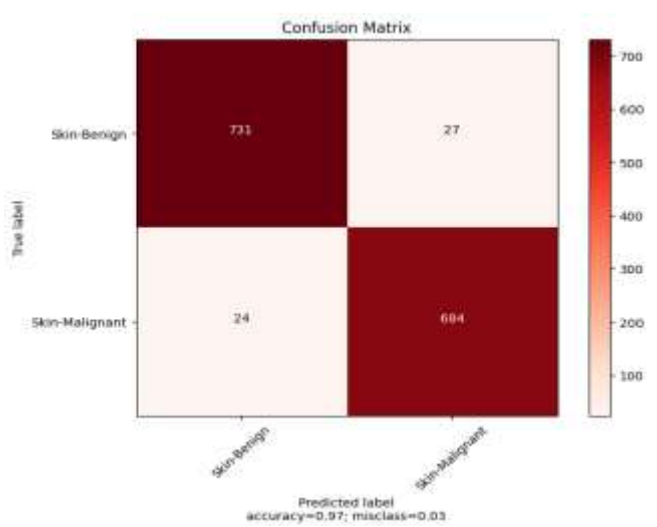


Figure 13: Confusion matrix representation of benign and malignant classification

**Figure** 13 illustrates the performance of the model that differentiates between benign and malignant skin lesions in the confusion matrix. The model properly identified 684 malignant and 731 benign skin lesions out of 700 total lesions. There were 27 misclassified malignant lesions, which were predicted to be benign, and 24 misclassified benign lesions, which were predicted to be malignant. With an accuracy of 97% overall, the classifier correctly categorized 97% of the skin lesions.

# 4.3 Comparison with Existing Models

To support the suggested method's feasibility, an effectiveness comparison with other methods was conducted. Table 1 demonstrates that our approach performed better than other networks. Within the suggested methodology, the Modified EfficientNet-B7 model was 96.63% accurate overall, outperforming the performance of the current models.

Proposed	Accurac	Precisio	Recall	F1-
Model	y	n		Scor
				e
ARDT-	0.857	0.756	0.816	-
DenseNets				
[5]				
VGG19 [2]	0.93	0.92	0.94	0.93
Stacked	0.957	0.95	0.96	0.96
model [1]				
Ensemble	0.92	0.91	0.92	0.92
(3 best				
models) [7]				
Inception-	0.86	0.8	0.89	0.84
v3 [10]				
Modified	0.9663	0.9644	0.968	0.96
EfficientNet			2	3
-B7				

Table 2: comparison of proposed model with other model

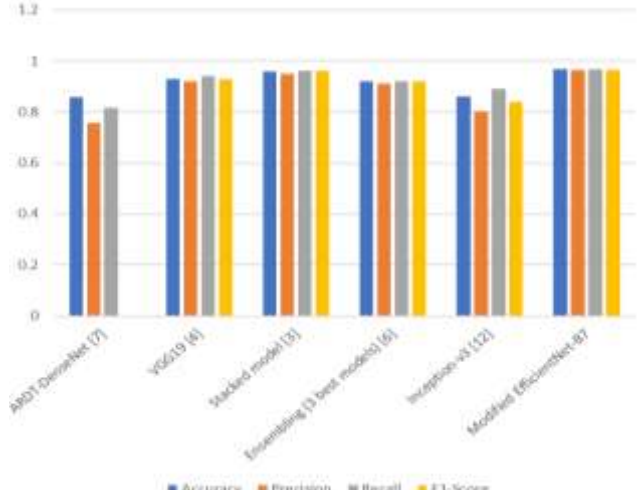


Figure 14: Comparison of Existing Neural Network
Architectures for skin cancer detection



#### CONCLUSION

The classification of skin cancer is crucial for both early diagnosis and effective treatment, particularly when utilizing state-of-the-art imaging methods sophisticated algorithms. The research takes a thorough strategy to improve the accuracy of the algorithm used to diagnose skin cancer, concentrating on important image acquisition, cleaning, enhancement, segmentation, and feature extraction. The integration of data augmentation techniques, encompassing noise, rotation, scaling, among others, is highlighted as a crucial step to improve model generalization. The study focuses on the use of the EfficientNetB7 model, which is prominent for its capacity to manage jobs requiring a high degree of accuracy and obtaining the benefits of larger and deeper neural networks. EfficientNetB7's performance metrics are remarkable when compared to other models, such as ARDT-DenseNet, VGG19, Stacked model, Ensembling, and Inception-v3. Notably, the model's efficacy in classifying skin cancer is highlighted by the acquired accuracy of 96.52%, precision of 96.44%, recall value of 96.82%, and F1 score of 96.3%. These results highlight the potential for improving skin cancer diagnosis through the use of sophisticated deep learning models, especially EfficientNetB7. Such models show potential for clinical applications, opening the door to more precise and effective detection of skin cancer subtypes, given their high accuracy and strong performance metrics. As technology continues to evolve, the integration of sophisticated algorithms into medical practices may lead to enhanced patient outcomes and contribute to the global efforts to combat skin cancer.

## **REFERENCES**

- [1] M. Shorfuzzaman, "An explainable stacked ensemble of deep learning models for improved melanoma skin cancer detection," Multimedia Systems, Apr. 2021, doi: <a href="https://doi.org/10.1007/s00530-021-00787-5">https://doi.org/10.1007/s00530-021-00787-5</a>.
- [2] J. V. Tembhurne, N. Hebbar, H. Y. Patil, and T. Diwan, "Skin cancer detection using ensemble of machine learning and deep learning techniques," Multimedia Tools and Applications, Feb. 2023, doi: https://doi.org/10.1007/s11042-023-14697-3.
- [3] W. Gouda, N. U. Sama, G. Al-Waakid, M. Humayun, and N. Z. Jhanjhi, "Detection of Skin Cancer Based on Skin Lesion Images Using Deep Learning," *Healthcare*, vol. 10, no. 7, Pp. 1-12,2022, doi: 10.3390/healthcare10071183.
- [4] I. A. Alfi, Md. M. Rahman, M. Shorfuzzaman, and A. Nazir, "A Non-Invasive Interpretable Diagnosis of Melanoma Skin Cancer Using Deep Learning and Ensemble Stacking of Machine Learning Models," Diagnostics, vol. 12, no. 3, p. 726, Mar. 2022, doi: <a href="https://doi.org/10.3390/diagnostics12030726">https://doi.org/10.3390/diagnostics12030726</a>.
- [5] J. Wu, W. Hu, Y. Wen, W. Tu, and X. Liu, "Skin

- Lesion Classification Using Densely Connected Convolutional Networks with Attention Residual Learning," Sensors, vol. 20, no. 24, p. 7080, Dec. 2020, doi: https://doi.org/10.3390/s20247080.
- [6] M. Naqvi, Syed Qasim Gilani, T. Syed, O. Marques, and H.-C. Kim, "Skin Cancer Detection Using Deep Learning—A Review," vol. 13, no. 11, pp. 1911–1911, May 2023, doi: https://doi.org/10.3390/diagnostics13111911.
- [7] S. Shah et al., "A comprehensive study on skin cancer detection using artificial neural network (ANN) and convolutional neural network (CNN)," Clinical eHealth, vol. 6, pp. 76–84, Dec. 2023, doi: <a href="https://doi.org/10.1016/j.ceh.2023.08.002">https://doi.org/10.1016/j.ceh.2023.08.002</a>.
- [8] S. Jinnai, N. Yamazaki, Y. Hirano, Y. Sugawara, Y. Ohe, and R. Hamamoto, "The Development of a Skin Cancer Classification System for Pigmented Skin Lesions Using Deep Learning," Biomolecules, vol. 10, no. 8, p. 1123, Jul. 2020, doi: https://doi.org/10.3390/biom10081123.
- [9] A. Bassel, A. B. Abdulkareem, Z. A. A. Alyasseri, N. S. Sani, and H. J. Mohammed, "Automatic Malignant and Benign Skin Cancer Classification Using a Hybrid Deep Learning Approach," Diagnostics, vol. 12, no. 10, p. 2472, Oct. 2022, doi: https://doi.org/10.3390/diagnostics12102472.
- [10] M. A. Farooq, A. Khatoon, V. Varkarakis, and P. Corcoran, "Advanced Deep Learning Methodologies for Skin Cancer Classification in Prodromal Stages," arXiv.org, Mar. 13, 2020. https://arxiv.org/abs/2003.06356 (accessed Jan. 04, 2024).
- [11] R. Gordon, "Skin Cancer: An Overview of Epidemiology and Risk Factors," *Seminars in Oncology Nursing*, vol. 29, no. 3, pp. 160–169, Aug. 2013
- [12] A. Ghosh, B. Soni, and Ujwala Baruah, "Transfer Learning-Based Deep Feature Extraction Framework Using Fine-Tuned EfficientNet B7 for Multiclass Brain Tumor Classification," *Arabian Journal for Science and Engineering*, Dec. 2023, doi: <a href="https://doi.org/10.1007/s13369-023-08607-w">https://doi.org/10.1007/s13369-023-08607-w</a>.
- [13] C. W. Rundle, M. Militello, C. Barber, C. L. Presley, H. R. Rietcheck, and R. P. Dellavalle, "Epidemiologic Burden of Skin Cancer in the US and Worldwide," *Current Dermatology Reports*, vol. 9, no. 4, pp. 309–322, Sep. 2020, doi: https://doi.org/10.1007/s13671-020-00311-4.
- [14] A. N. Hoshyar, A. Al-Jumaily, and A. N. Hoshyar, "The Beneficial Techniques in Preprocessing Step of Skin Cancer Detection System Comparing," *Procedia Computer Science*, vol. 42, pp. 25–31, 2014, doi:



#### https://doi.org/10.1016/j.procs.2014.11.029.

- [15] T.-C. Pham, C.-M. Luong, M. Visani, and V.-D. Hoang, "Deep CNN and Data Augmentation for Skin Lesion Classification," *Intelligent Information and Database Systems*, pp. 573–582, 2018, doi: https://doi.org/10.1007/978-3-319-75420-8\_54.
- [16] M. Dildar *et al.*, "Skin Cancer Detection: A Review Using Deep Learning Techniques," *International Journal of Environmental Research and Public Health*, vol. 18, no. 10, p. 5479, May 2021, doi: https://doi.org/10.3390/ijerph18105479.
- [17] C. Supriyanto, A. Salam, J. Zeniarja, and A. Wijaya, "Two-Stage Input-Space Image Augmentation and Interpretable Technique for Accurate and Explainable Skin Cancer Diagnosis," *Computation*, vol. 11, no. 12, p. 246, Dec. 2023, doi: https://doi.org/10.3390/computation11120246.
- [18] O. Shridhar Murumkar, "Feature Extraction for Skin Cancer Lesion Detection." Accessed: Jan. 07, 2024. [Online]. Available: <a href="http://ijsetr.com/uploads/136524IJSETR4388-297.pdf">http://ijsetr.com/uploads/136524IJSETR4388-297.pdf</a>
- [19] A. Bhattacharya, A. Young, A. Wong, S. Stalling, M. Wei, and D. Hadley, "Precision Diagnosis Of Melanoma And Other Skin Lesions From Digital Images," *AMIA Summits on Translational Science Proceedings*, vol. 2017, pp. 220–226, Jul. 2017, Available: https://www.ncbi.nlm.nih.gov/pmc/articles/PMC554338
- https://www.ncbi.nlm.nih.gov/pmc/articles/PMC554338 7/
- [20]"ISIC Archive," www.isic-archive.com. https://www.isic-archive.com/
- [21] "Skin Cancer ISIC," www.kaggle.com. <a href="https://www.kaggle.com/datasets/nodoubttome/skin-cancer9-classesisic">https://www.kaggle.com/datasets/nodoubttome/skin-cancer9-classesisic</a>
- [22]Chandana, S., Nagarathna, C. R., Amrutha, A., & Jayasri, A. (2024, January). Detection of image forgery using error level analysis. In 2024 International Conference on Intelligent and Innovative Technologies in Computing, Electrical and Electronics (IITCEE) (pp. 1-5). IEEE.
- [23] Bhavyashree, H. L., Nagarathna, C. R., Preetham, A., & Priyanka, R. (2019, March). Modified cluster based certificate blocking of misbehaving node in MANETS. In 2019 1st international conference on advanced technologies in intelligent control, environment, computing & communication engineering (ICATIECE) (pp. 155-161). IEEE.
- [23] A. N. Hoshyar, A. Al-Jumaily, and A. N. Hoshyar, "The Beneficial Techniques in Preprocessing Step of Skin Cancer Detection System Comparing," *Procedia Computer Science*, vol. 42, pp. 25–31, 2014, doi:

#### https://doi.org/10.1016/j.procs.2014.11.029.

- [24]Preetham, A., Vyas, S., Kumar, M., & Kumar, S. N. P. (2024). Optimized convolutional neural network for land cover classification via improved lion algorithm. *Transactions in GIS*, 28(4), 769-789.
- [25] Preetham, A., & Battu, V. V. (2023). Soil Moisture Retrieval Using Sail Squirrel Search Optimization-based Deep Convolutional Neural Network with Sentinel-1 Images. *International Journal of Image and Graphics*, 23(05), 2350048.
- [26] A. Patil, Y. S. Ingle, N. F. Shaikh, P. N. Mahalle, and J. Barot, "Skin Cancer Image Augmentation Techniques Using AI: A Survey of the State-of-the-Art," *Lecture notes in networks and systems*, pp. 569–579, Jan. 2023, doi: <a href="https://doi.org/10.1007/978-981-99-4932-8">https://doi.org/10.1007/978-981-99-4932-8</a> 52.
- [27] Nagarathna, C. R., & Kusuma, M. M. (2023). Early detection of Alzheimer's Disease using MRI images and deep learning techniques. *Alzheimer's & Dementia*, 19, e062076.
- [28] Nagarathna, C. R., Bhagya, K. G., Devaraju, H. B., Somashekara, A. S., & Kishore, H. N. (2025). Machine Learning Techniques for EEG-Based Alzheimer's Disease Classification. Mathematical Modelling of Engineering Problems, 12(3).
- [29] "Efficient Processing of Deep Neural Networks: A Tutorial and Survey," *ieeexplore.ieee.org*. https://ieeexplore.ieee.org/abstract/document/8114708/
- [30] K. O'Shea and R. Nash, "An Introduction to Convolutional Neural Networks," *arXiv:1511.08458* [cs], Dec. 2015, Available: <a href="https://arxiv.org/abs/1511.08458">https://arxiv.org/abs/1511.08458</a>
- [31] V. Agarwal, "Complete Architectural Details of all EfficientNet Models," *Medium*, May 31, 2020. <a href="https://towardsdatascience.com/complete-architectural-details-of-all-efficientnet-models-5fd5b736142">https://towardsdatascience.com/complete-architectural-details-of-all-efficientnet-models-5fd5b736142</a>
- [32]Nagamalla, V., Kumar, B. M., Janu, N., Preetham, A., Parambil Gangadharan, S. M., Alqahtani, M. A., & Ratna, R. (2022). Detection of adulteration in food using recurrent neural network with internet of things. *Journal of Food Quality*, 2022(1), 6163649.
- [33] Preetham, A., & Almas, M. (2023). Alzheimer's Classification from EGG Signals Employing Machine Learning Algorithms. Journal of Electronics and Informatics, 5(4), 386-404.
- [34] Nagarathna, C. R., & Mohanchandra, K. (2023). An overview of early detection of Alzheimer's disease. International Journal of Medical Engineering and Informatics, 15(5), 442-457.
- [35] Rangegowda, N. C., Mohanchandra, K., Preetham,



- A., Almas, M., & Huliyappa, H. (2023). A Multi-Layer Perceptron Network-Based Model for Classifying Stages of Alzheimer's Disease Using Clinical Data. Revue d'Intelligence Artificielle, 37(3), 601.
- [36] K. Team, "Keras documentation: EfficientNet B0 to B7," *keras.io*. https://keras.io/2.15/api/applications/efficientnet/ (accessed Jan. 07, 2024).
- [37] A. Suresh, "What is a confusion matrix?," *Medium*, Nov. 20, 2020. <a href="https://medium.com/analytics-vidhya/what-is-a-confusion-matrix-d1c0f8feda5">https://medium.com/analytics-vidhya/what-is-a-confusion-matrix-d1c0f8feda5</a>
- [38] K. Ali, Z. A. Shaikh, A. A. Khan, and A. A. Laghari, "Multiclass skin cancer classification using EfficientNets a first step towards preventing skin cancer," *Neuroscience Informatics*, vol. 2, no. 4, p. 100034, Dec. 2022, doi: https://doi.org/10.1016/j.neuri.2021.100034.
- [39] S. McCombes, "Sampling Methods | Types and Techniques Explained," *Scribbr*, Sep. 19, 2019.
  [40] American Academy of Dermatology Association, "Types of skin cancer," *www.aad.org*. <a href="https://www.aad.org/public/diseases/skin-cancer/types/common">https://www.aad.org/public/diseases/skin-cancer/types/common</a>
- [41] M. Tan and Q. Le, "EfficientNet: Rethinking Model Scaling for Convolutional Neural Networks," *proceedings.mlr.press*, May 24, 2019. <a href="http://proceedings.mlr.press/v97/tan19a.html?ref=jina-ai-gmbh.ghost.io">http://proceedings.mlr.press/v97/tan19a.html?ref=jina-ai-gmbh.ghost.io</a> 2024;25(3):98. Published 2024 Mar 8. doi:10.31083/j.rcm2503098
- [42] Chou PS, Ho BL, Chan YH, Wu MH, Hu HH, Chao AC. Delayed diagnosis of atrial fibrillation after first-ever stroke increases recurrent stroke risk: a 5-year nationwide follow-up study. Intern Med J. 2018 Jun;48(6):661-667.
- [43] Hannun AY, Rajpurkar P, Haghpanahi M, et al. Cardiologist-level arrhythmia detection and classification in ambulatory electrocardiograms using a deep neural network. Nat Med. 2019;25(1):65-69.
- [44]. Abbas Q, Jeong W, Lee SW. Explainable AI in Clinical Decision Support Systems: A Meta-Analysis of Methods, Applications, and Usability Challenges. Healthcare (Basel). 2025;13(17):2154. Published 2025 Aug 29.
- [45] El Arab RA, Abu-Mahfouz MS, Abuadas FH, et al. Bridging the Gap: From AI Success in Clinical Trials to Real-World Healthcare Implementation-A Narrative Review. Healthcare (Basel). 2025;13(7):701. Published 2025 Mar 22.